BNL-67393-AB

T. B. Onasch, R. McGraw, A. J. Prenni, M. A. Tolbert, and D. Imre

April 2000

Extended Abstract for presentation at the
15th International Conference on Nucleation and Atmospheric Aerosols,
Hosted by the Cloud and Aerosol Sciences Laboratory and
the Physics Department, University of Missouri-Rolla
Rolla, Missouri
August 6-11, 2000

Efflorescence and ice nucleation in ammonium sulfate particles: Analysis of experimental results using scaled nucleation theory

T. B. Onasch[1], R. McGraw[1], A. J. Prenni[2], M. A. Tolbert[2] and D. Imre[1]

[1]*Brookhaven National Laboratory, Atmospheric Sciences Division, Environmental Sciences Department, Upton, NY 11973*
[2]*University of Colorado, Department of Chemistry and Biochemistry and CIRES, Boulder, CO 80309*

Abstract. Temperature-dependent efflorescence and ice nucleation results of ammonium sulfate aerosol obtained from flow tube studies are analyzed using a newly developed model based on scaled nucleation theory. The presented thermodynamic model defines trajectories of constant reduced nucleation barrier height as a function of temperature and yields simple analytic expressions for the liquid-solid nucleation boundaries. Within the context of the model the experimental results are interpreted in terms of surface enthalpy, entropy and nucleus size. These thermodynamic properties, along with a full thermodynamic model, can be then used to predict changes in the composition and phase of ammonium sulfate particles over the wide range of relative humidity and temperature conditions found in the atmosphere.

INTRODUCTION

In this paper we describe a thermodynamic model of homogeneous liquid-solid nucleation based on the Gibbs dividing surface model of a nucleus and apply it to experimental ammonium sulfate aerosol data. This model relies on the use of scaling forms for such physical quantities as surface tension, density, and temperature to nondimensionalize the nucleation barrier height [1, 2, 3]. The model yields compact analytical expressions for trajectories of constant reduced barrier height, and therefore, because the effect of the kinetic prefactor is less, essentially constant nucleation rate [2]. Some advantages of this approach are that the scaled quantities are fewer in number and tend to show considerably less variability than, for example, the cube of the surface tension that appears in the barrier height in the classical nucleation theory.

Ammonium sulfate aerosol was selected for study because it is a major component of the atmospheric aerosol and its phase transformation properties are of considerable importance to atmospheric chemistry and climate. The equilibrium and metastability phase diagrams have been rigorously investigated [4, 5, 6, 7] and thermodynamic models developed [8]. Thus the ammonium sulfate aerosol system provides an excellent model for the development and testing of new approaches to liquid-solid nucleation.

FLOW TUBE EXPERIMENTS

Deliquescence, efflorescence and ice nucleation experiments have been carried out on small (submicrometer) ammonium sulfate aerosol in a temperature-controlled flow tube system [4, 5]. Large supercoolings are readily and reproducibly achieved in these freely floating aerosol droplets. Reproducibility of a well defined supercooling limit, together with the absence of heterogeneous nucleation sites, suggests that the limit to supercooling is determined by homogeneous nucleation. The temperature-controlled flow tube system has been described elsewhere [4, 5]. An FTIR spectrometer is used for estimating the size distribution and the phase transitions of the ammonium sulfate particles. The relative humidity in the flow tube was controlled by conditioning the aerosol flow using sulfuric acid solutions and ice coated walls. The relative humidity was directly measured by FTIR and by a dew point hygrometer for the efflorescence study, and calculated from the temperature of the ice-coated walls for the ice nucleation experiments. The experiments yielded accurate determinations of the deliquescence and efflorescence points, and ice nucleation thresholds, as a functions of aerosol temperature and relative humidity (RH).

THERMODYNAMICS

Following the standard thermodynamic treatment of binary solutions [9] we obtain the following equation relating the vapor pressure of water $p1$, the mole fractions of water and salt in solution (x_1 and x_2, respectively), and the driving free energy for salt crystallization ($\Delta\mu_2 = kT\ln S_2$, where S_2 is the saturation ratio for salt in solution relative to the crystalline phase):

$$\frac{d\ln p_1}{dT} + \frac{x_2}{x_1}\frac{d(\Delta\mu_2/kT)}{dT} = -\frac{\Delta H_v}{kT^2} - \frac{x_2}{x_1}\frac{\Delta H_s}{kT^2}. \tag{1}$$

For pure water, $x_2=0$ and Eq.1 reduces to the familiar Clausius-Clapeyron relation where ΔHv is the heat of vaporization. For a saturated salt solution, $\Delta\mu_2=0$ and Eq. 1 describes the vapor pressure along the (equilibrium) deliquescence line where ΔH_s is the integral heat of solution [7].

In terms of the driving free energy for ice crystallization ($\Delta\mu_1 = kT\ln S_1$, where S_1 is the saturation ratio of water vapor relative to ice), we obtain:

$$\frac{d\ln p_1}{dT} + \frac{d(\Delta\mu_1/kT)}{dT} = -\frac{\Delta H_v}{kT^2} - \frac{\Delta H_{melt}}{kT^2}, \tag{2}$$

where ΔH_{melt} is the heat of melting. For ice in equilibrium with water vapor, $\Delta\mu_1=0$, and Eq. 2 relates the equilibrium water vapor pressure over ice to the heat of sublimation.

Figure 1 shows $\ln p_1$ versus $1/T$ curves for pure water and ice [8], and experimental data for deliquescence and efflorescence of salt, and ice nucleation. Lines through the

data points are linear fits. The two upper curves on the left side of the figure correspond to the two special cases of Eq.1 described above. The dashed curve corresponds to the special ice sublimation case of Eq. 2. The lower (efflorescence) curve on the left also corresponds to a special case of Eq. 1 - that for which $\Delta\mu_2$ assumes values marking the salt nucleation threshold. In similar fashion, the ice nucleation curve (upper right curve) corresponds to a special case of Eq. 2 -that for which $\Delta\mu_1$ assumes values marking the ice nucleation threshold. In the following section we describe trajectories for $\Delta\mu_1$ and $\Delta\mu_2$ at the homogeneous nucleation thresholds for ice nucleation and salt nucleation, respectively. We obtain these trajectories solely in terms of the molecular properties of the critical nucleus using the Gibbs dividing surface model and scaled nucleation theory of Hale [3].
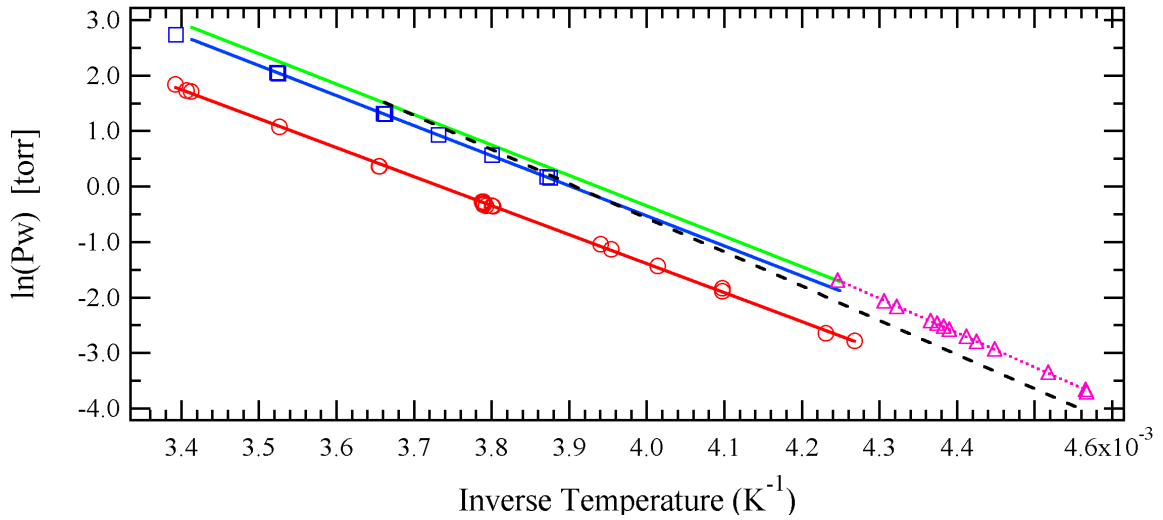
FIGURE 1. Plot of the equilibrium and metastable phase transitions for ammonium sulfate. The solid line is the vapor pressure of water over pure liquid water and the dashed line is the vapor pressure of water over ice, both derived from Clegg et al. [8]. The squares are the deliquescence data, the circles are the efflorescence transition [4] and the triangles are the ice nucleation data [5].

SCALED NUCLEATION THEORY

Throughout this section $\Delta\mu$ and S will refer to either component and γ_s is the interfacial free energy, per unit area, between the nucleus (either salt or ice) and the parent solution. We begin with the following trajectory equation for $\Delta\mu$, which defines a path of fixed nucleation barrier height (or approximately constant nucleation rate):

$$\frac{d\Delta\mu}{dT} = \frac{3}{2}\Delta\mu\left(\frac{1}{\gamma_s}\frac{d\gamma_s}{dT}\right) - \frac{\Delta\mu}{2T}. \tag{3}$$

Eq. 3 assumes that the nucleus is incompressible and has a temperature-independent density. Transforming to the $\ln S$ coordinate gives:

$$\frac{d(\Delta\mu/kT)}{dT} = \frac{d\ln S}{dT} = -\frac{1}{kT^2}\frac{A_s}{n_f^*}\left(\gamma_s - T\frac{d\gamma_s}{dT}\right) = -\frac{1}{kT^2}\frac{\Delta H_{surface}}{n_f^*} \qquad (4)$$

where $\Delta H_{surface}$ is the total surface enthalpy and n_f^* is the number of molecules within the critical nucleus boundary defined by the surface of tension (surface area A_s). Eqs. 3 and 4 are not new and can be found in papers of Ford [10] and earlier, in very similar form, in the scaled nucleation theory of Hale [3]. Their derivation using the Gibbs-dividing surface model, is described in this proceedings [1].

Substitution of Eq. 4 into Eqs. 1 and 2 yields thermodynamic conditions along a phase-space trajectory of constant nucleation rate. Note that the right hand side of Eq. 4 contains the total surface enthalpy divided by the number of molecules in the nucleus. The closeness in slopes of the linear fits in Fig. 1 suggest that this quantity is small compared to the enthalpies per molecule of vaporization and sublimation.

Eq. 3 is a remarkably simple and elegant expression for the nucleation threshold conditions. It implies that an entire nucleation threshold trajectory can be generated using only bulk solution properties and an estimate for $\gamma_s^{-1}d\gamma_s/dT$. The latter quantity is the relative slope of the Eötvös line, describing the empirical linear relation between surface tension and temperature [11]. It is clearly much less sensitive to uncertainty in γ_s then is the nucleation rate itself, or even the exponent of the nucleation rate.

As an example, the surface tension between an ice nucleus and the ammonium sulfate solution has been estimated using Antonoff's rule. The derived per-unit-area surface entropy and surface enthalpy are found to be independent of temperature, in agreement with Eötvös rule [11]. Nucleation trajectories based on the derived surface tension are compared with the experimentally determined ice nucleation data.

REFERENCES

1. R. McGraw, Scaling properties of critical nuclei and nucleation rates, 15th International Conference on Nucleation and Atmospheric Aerosols, University of Missouri - Rolla (2000).
2. R. McGraw, Journal of Chemical Physics 75, 5514 (1981).
3. B. N. Hale, Lecture Notes in Physics, P. E. Wagner, G. Vali, Eds., 12th International Conference on Nucleation and Atmospheric Aerosols, University of Vienna - Austria (1988).
4. T. B. Onasch, et al., Journal of Geophysical Research 104, 21,317-21,326 (1999).
5. A. J. Prenni, M. E. Wise, S. D. Brooks, M. A. Tolbert, Submitted to Journal of Geophysical Research (2000).
6. J. Xu, D. Imre, R. McGraw, I. Tang, The Journal of Physical Chemistry B. 102, 7462-7469 (1998).
7. I. N. Tang, H. R. Munkelwitz, Atmospheric Environment 27A, 467-483 (1993).
8. S. L. Clegg, P. Brimblecombe, A. S. Wexler, Journal of Physical Chemistry 102A, 2137-2154 (1998).
9. E. A. Guggenheim, in Thermodynamics . (North-Holland, Amsterdam, 1959) pp. 296.
10. J. Ford, Journal of Chemical Physics 105, 8324-8332 (1996).
11. A. B. Pippard, in Elements of classical thermodynamics for advanced students of physics . (Cambridge University Press, Cambridge, 1957) pp. 86.